Published in final edited form as:
Cancer Cell. 2006 July ; 10(1): 51–64. doi:10.1016/j.ccr.2006.06.001.

Autophagy promotes tumor cell survival and restricts necrosis, inflammation, and tumorigenesis

Kurt Degenhardt[1,2,3,10], **Robin Mathew**[1,9,10], **Brian Beaudoin**[1,3,10], **Kevin Bray**[2,3,4], **Diana Anderson**[3], **Guanghua Chen**[1,3,5], **Chandreyee Mukherjee**[1,3,5], **Yufang Shi**[6,9], **Céline Gélinas**[1,8,9], **Yongjun Fan**[1], **Deirdre A. Nelson**[5], **Shengkan Jin**[7,9], and **Eileen White**[1,2,3,4,9,*]

[1] Center for Advanced Biotechnology and Medicine, 679 Hoes Lane, Piscataway, New Jersey 08854

[2] Department of Molecular Biology and Biochemistry, Rutgers University, 604 Allison Road, Piscataway, New Jersey 08854

[3] Rutgers University, 679 Hoes Lane, Piscataway, New Jersey 08854

[4] Cancer Institute of New Jersey, 195 Little Albany Street, New Brunswick, New Jersey 08903

[5] Howard Hughes Medical Institute, 4000 Jones Bridge Road, Chevy Chase, Maryland 20815

[6] Department of Molecular Genetics, Microbiology and Immunology, University of Medicine and Dentistry of New Jersey, Robert Wood Johnson Medical School, 675 Hoes Lane, Piscataway, New Jersey 08854

[7] Department of Pharmacology, University of Medicine and Dentistry of New Jersey, Robert Wood Johnson Medical School, 675 Hoes Lane, Piscataway, New Jersey 08854

[8] Department of Biochemistry, University of Medicine and Dentistry of New Jersey, Robert Wood Johnson Medical School, 675 Hoes Lane, Piscataway, New Jersey 08854

[9] University of Medicine and Dentistry of New Jersey, Robert Wood Johnson Medical School, 675 Hoes Lane, Piscataway, New Jersey 08854

Summary

Defective apoptosis renders immortalized epithelial cells highly tumorigenic, but how this is impacted by other common tumor mutations is not known. In apoptosis-defective cells, inhibition of autophagy by AKT activation or by allelic disruption of *beclin1* confers sensitivity to metabolic stress by inhibiting an autophagy-dependent survival pathway. While autophagy acts to buffer metabolic stress, the combined impairment of apoptosis and autophagy promotes necrotic cell death in vitro and in vivo. Thus, inhibiting autophagy under conditions of nutrient limitation can restore cell death to apoptosis-refractory tumors, but this necrosis is associated with inflammation and accelerated tumor growth. Thus, autophagy may function in tumor suppression by mitigating metabolic stress and, in concert with apoptosis, by preventing death by necrosis.

*Correspondence: ewhite@cabm.rutgers.edu.
[10]These authors contributed equally to this work.

Supplemental data
The Supplemental Data include Supplemental Experimental Procedures and two supplemental figures and can be found with this article online at http://www.cancercell.org/cgi/content/full/10/1/51/DC1/.

Introduction

Defects in type I programmed cell death or apoptosis perturb development, promote tumorigenesis, and impair chemotherapy, suggesting that diversion to an alternative cell death pathway such as autophagy or necrosis in these circumstances may be therapeutically beneficial. Apoptosis is a well-defined process of cellular dismantling that leads to cell corpses that are engulfed by phagocytosis in the absence of an inflammatory response and is a means for cell elimination in development (Adams, 2003; Danial and Korsmeyer, 2004). BCL-2 family proteins are key regulators of apoptosis that are represented by antiapoptotic proteins, such as BCL-2, and proapoptotic BAX and BAK, which regulate the efflux of proapoptotic molecules from mitochondria and other organelles. Deficiency in BAX and BAK or expression of BCL-2 blocks apoptosis, and this failure to execute apoptotic cell death effects development and promotes tumorigenesis. As BCL-2 has no additional tumor-promoting function in the absence of BAX and BAK, inhibition of the BAX/BAK apoptotic pathway is the means by which BCL-2 enables tumor growth (Degenhardt et al., 2002a; Nelson et al., 2004; Tan et al., 2005).

Autophagy, or type II programmed cell death, is a catabolic process whereby cells self-digest intracellular organelles; however, when allowed to go to completion, autophagy is a means of achieving cell death (Edinger and Thompson, 2003; Levine, 2005). Autophagy is an evolutionarily conserved, genetically controlled process that results in the targeting of cellular proteins and organelles to lysosomes for degradation. This may serve to regulate normal turnover of organelles and to remove those with compromised function to maintain homeostasis. However, autophagy can also be considered a temporary survival mechanism during periods of starvation where self-digestion provides an alternative energy source and also may facilitate the disposal of unfolded proteins under stress conditions (Kamatsu et al., 2005; Kuma et al., 2004). Autophagy is controlled by mTOR downstream of PI-3 kinase/AKT, which regulates cell growth and protein synthesis in response to nutrient and growth factor availability. The catabolic function provided by autophagy is thereby suppressed when the external nutrient supply is adequate to support cellular metabolism. Defects in autophagy profoundly perturb development, and although haploinsufficiency in the essential autophagy gene *beclin1* promotes tumorigenesis, the mechanism is not known (Liang et al., 1999; Qu et al., 2003; Yue et al., 2003).

A third means to achieve cell death is by necrosis, which usually is associated with physical insults, failure of osmotic regulation, ATP depletion, HMGB1 release, cell lysis, and an inflammatory response that may facilitate wound healing (Kanduc et al., 2002; Majno and Joris, 1995; Nelson and White, 2004; Proskuryakov and Konoplyannikov, 2003; Zeh and Lotze, 2005; Zong and Thompson, 2006). Although necrotic cell death is not considered to be under genetic control, regulators of ATP availability such as poly-ADP-ribose polymerase determine the propensity for necrosis and may link necrosis to metabolic function. Finally, necrosis is a common feature of human tumors and is associated with poor prognosis; however, the cause of necrosis and its effects on tumor growth are not known.

We have identified an oncogene-activated pathway for necrotic cell death in response to metabolic (ischemic) stress. This pathway to necrosis requires inhibition of the primary default mechanism of cell death, apoptosis, and occurs by inhibition of an autophagy-dependent survival mechanism that sustains normal cell function and viability during energy deprivation. Thus, coordinate genetic inactivation of apoptosis and autophagy enables death by necrosis, suggesting that a functional relationship exists among different death pathways to limit necrosis. Indeed, necrosis produces an inflammatory response that is associated with enhanced tumor growth. Thus, necrotic cell death can be genetically controlled, and there are functional interactions between the three cell death mechanisms. Understanding how

different forms of cell death are controlled, are interdependent, and impact the tumor microenvironment may yield insight into their role in cancer and into the development of effective therapies.

Results

AKT promotes epithelial tumorigenesis in the presence and absence of a functional apoptotic pathway

To determine the role of the AKT pathway in epithelial tumorigenesis and the functional relationship with apoptosis, immortalized baby mouse kidney epithelial (iBMK) cells that express BAX/BAK (W2) or that are BAX/BAK-deficient (D3) (Degenhardt et al., 2002b) were engineered to stably express either a constitutively active form of AKT (*myr*-AKT) or RAS (H-ras^{V12}). Several RAS- and AKT-expressing stable clones were derived from both W2 and D3 parental iBMK cell lines, along with vector controls. All express E1A and p53DD, whereas BAX and BAK are expressed only in W2 (Figure 1A; data not shown; Tan et al., 2005). To assess the tumorigenic capacity of W2 and D3 cells expressing either activated RAS or AKT, cells were injected subcutaneously into nude mice.

The vector control W2 cells (W2 3.1.2, 5, and 6) were poorly tumorigenic with clonal tumor growth occurring beyond 3 months postinjection (Figure 1B) (Degenhardt et al., 2002a; Nelson et al., 2004; Tan et al., 2005). Failure of W2 cells to establish tumors efficiently in vivo is attributed to ischemic conditions following implantation in vivo that result in BIM-dependent, BAX/BAK-mediated apoptosis that largely eliminates W2 cells (Nelson et al., 2004; Tan et al., 2005). In contrast, RAS rendered W2 cells highly tumorigenic, with tumors forming within 16 days, remarkably faster than BAX/BAK-deficient D3 cells (Figure 1B), where an apoptotic block enables tumor growth within 30–60 days (Degenhardt et al., 2002a; Nelson et al., 2004; Tan et al., 2005). Interestingly, RAS enhanced D3 tumor growth, indicating a tumor-promoting function independent of apoptosis regulation (Figure 1B). AKT promoted W2 tumor growth, although less so than RAS (Figure 1B). In contrast, AKT dramatically enhanced D3 tumor growth to nearly that of RAS (Figure 1B). Although AKT promotes cell survival, AKT-mediated acceleration of tumor growth in BAX/BAK-deficient cells indicates a tumor-promoting activity independent of apoptosis inhibition. Indeed, AKT synergizes with antiapoptotic BCL-x_L to promote leukemogenesis (Karnauskas et al., 2003) and has prominent roles in regulating cell growth and metabolism that contribute to tumorigenesis (Hanada et al., 2004). Given the importance of the PI3 kinase/AKT pathway in human tumorigenesis, it was of interest to identify the apoptosis-independent function of AKT that enhanced solid tumor growth observed here.

AKT promotes tumor necrosis associated with metabolic stress when apoptosis is disabled

To examine the mechanism of enhanced tumor growth by AKT, tumors were examined histologically by hematoxylin and eosin (H&E) and immunohistochemistry (IHC). Late-forming tumors derived from W2 cells are invasive carcinomas with a high mitotic rate (P-H3 staining), isolated areas of necrosis, and scattered active caspase-3-positive apoptotic cells (Figure 1C; Figure S1 in the Supplemental Data available with this article online) (Nelson et al., 2004). D3 tumors are invasive carcinomas with a high mitotic rate and prevalent polyploid tumor giant cells (Figure 1C; Figure S1) (Degenhardt et al., 2002a; Nelson et al., 2004). Isolated necrotic areas are found, but no apoptosis occurs, as indicated by an absence of active caspase-3 (Figure S1) (Nelson et al., 2004). Evidence suggests that ischemic conditions in the tumor microenvironment result in mitotic slippage or adaptation to generate ploidy abnormalities in tumor cells that are preserved by an apoptotic defect (Nelson et al., 2004).

AKT enabled W2 cells to form carcinomas with a high mitotic rate without tumor giant cells (Figure 1C; Figure S1). Surprisingly, and in contrast to the D3 tumors, D3 AKT tumors (and also D3 RAS) were largely necrotic. Viable D3 AKT tumor cells were apparent in a striking growth pattern surrounding blood vessels in layers approximately ten cells deep (Figure 1C). Radiating outward from the regions of viable tumor was a layer of necrotic cells typified by condensed disk-shaped nuclei and eosinophilic (pink) cytoplasm, which were followed by areas of cell debris with possible infiltrating host cells (see below) (Figure 1C). In contrast to D3 tumors that were nearly entirely composed of viable tumor cells, roughly half the volume of D3 AKT and D3 RAS tumors was necrotic. Furthermore, hypoxic conditions localized to necrotic areas of D3 AKT tumors, neither of which were present in D3 tumors (Figure 1D), suggesting that necrosis in vivo was associated with metabolic stress.

IHC for active caspase-3 (Nelson et al., 2004) indicated scant evidence of apoptosis in D3, D3 AKT, and D3 RAS tumors, although necrotic areas of D3 AKT and D3 RAS tumors showed active caspase-3 positive cells of undetermined origin, possibly tumor or infiltrating host cells (Figure S1). W2 (Nelson et al., 2004), W2 AKT, and W2 RAS tumors displayed active caspase-3 scattered throughout tumor tissue (Figure S1). Furthermore, AKT activation in tumors where apoptosis was inhibited by BCL-2 were necrotic, indicating that promotion of necrosis was independent of the means of apoptosis inactivation (Figure 1E). Thus, activation of AKT or RAS stimulated tumor growth but also activated cell death by necrosis specifically in tumors possessing an apoptotic defect and in association with metabolic stress. Finally, the necrotic tumor phenotype was not merely a reflection of rapid growth, as RAF activation (RAF-CAAX) similarly promoted D3 tumor growth but without necrosis (data not shown). This suggests that AKT activation can profoundly sensitize apoptosis-defective tumors to necrotic cell death.

AKT activation in apoptosis-defective cells stimulates necrosis in response to metabolic stress in vitro

To test the hypothesis that metabolic stress in tumors in vivo was the stimulus for not only apoptotic cell death in W2 cells, but also necrotic cell death in D3 AKT cells, iBMK cell lines were subjected to ischemia in vitro. W2, W2 AKT, D3, and D3 AKT iBMK cell lines were either untreated or incubated in a 1% oxygen gas mixture and no glucose that simulates ischemic conditions in the tumor microenvironment (Nelson et al., 2004), and cells were analyzed by flow cytometry. While all four cell line genotypes displayed a normal cell cycle profile when untreated, apoptotic cell death occurred, indicated by the increase in the sub-G1 population in treated W2 and W2 AKT cells and activation of caspase-3 (Figures 2A and 2B). Although AKT can block apoptosis, this does not occur in ischemia, since AKT requires glucose to inhibit apoptosis (Gottlob et al., 2001; Plas et al., 2001). In contrast, apoptosis-defective D3 cells remained viable in ischemia, and cells accumulated at G2/M and beyond (Figure 2A) (Nelson et al., 2004) without activating caspase-3 (Figure 2B). D3 AKT cells, however, lost viability in ischemia due to cellular disintegration without stimulation of caspase-3 activation (Figures 2A and 2B). The dramatic induction of cell death by AKT in D3 cells required both glucose and oxygen deprivation, as deprivation of either alone was substantially less effective. This was also observed by trypan blue staining in multiple independent cell lines (data not shown). Electron microscopy (EM) under normal and ischemic conditions revealed apoptotic morphology in ischemic W2 and W2 AKT cells, and necrosis of ischemic D3 AKT cells as indicated by vacuolated cytoplasm (Figure 2C) coincident with release of the necrotic marker HMGB1 (Scaffidi et al., 2002) from nuclei (Figure 2D). Thus, cell death triggered by AKT activation in BAX/BAK-deficient cells under metabolic stress resembles necrosis and not apoptosis, which sensitized these normally death-resistant cells to cell death.

Strikingly, D3 cells under ischemia displayed a highly unusual ultrastructural morphology consisting of the accumulation of double membrane vesicles containing cytoplasmic organelles indicative of autophagy (Figure 2C) while retaining nuclear HMGB1 (Figure 2D). Autophagy can be a method of cell death if allowed to proceed to completion; however, it is also a mechanism for prolonging survival in response to nutrient depletion by permitting the utilization of a cell-internal energy source. This suggested that cells apoptose in response to ischemia, but that defective apoptosis permits sustained autophagy possibly to support survival that may be compromised by AKT activation.

AKT inhibits autophagy-mediated survival in ischemia

To quantitate the level of autophagy induced by ischemia in D3 compared to D3 AKT cells, cytosol to membrane translocation of the autophagy marker EGFP-LC3 was monitored (Mizushima et al., 2004; Tanida et al., 2004). Both D3 and D3 AKT cells displayed predominantly diffuse EGFP-LC3 localization under normal growth conditions (Figure 3A). In ischemia there was a dramatic shift in the distribution of EGFP-LC3 from diffuse to punctate localization, indicative of lipidation and membrane translocation in D3 cells that was substantially delayed in D3 AKT cells (Figures 3A and 3B). By 48 hr of ischemia, the percentage of translocated EGFP-LC3 in D3 AKT cells approximated that in D3 cells (Figure 3B), but by that time the viability of D3 AKT cells was less than 10% compared to 90% in D3 cells (Figure 2A; data not shown). Similar results were obtained by examining lipidation of endogenous LC3 (data not shown). Thus, in the background of an apoptosis defect, AKT activation impairs autophagy induction in response to metabolic stress, potentially eliminating a survival mechanism resulting in necrosis.

Autophagy was also induced by ischemia prior to apoptosis in W2 cells (from 3% to 57% at 6 hr of ischemia), and impaired induction of autophagy was observed in W2 AKT cells (from 10% to 20% at 6 hr of ischemia). In apoptosis-competent cells, starvation induces both autophagy and apoptosis; however, W2 and W2 AKT undergo apoptosis at equal rates (Figure 2A), suggesting that the induction of autophagy does not delay or prevent apoptosis and that apoptosis prevails over autophagy. In contrast to normal cells (cardiac cells under neonatal starvation, for example) where autophagy may delay or prevent apoptosis, oncogene activation predisposes cancer cells to apoptosis that may not allow survival by autophagy.

Knockdown of autophagy promotes sensitivity to metabolic stress

To test if autophagy is the mechanism used by D3 cells to survive ischemia, the expression of the essential autophagy gene *beclin1* was knocked down using RNAi, and the impact on cell viability under ischemic conditions was determined. RNAi effectively reduced Beclin1 protein levels relative to the LaminA/C control (Figure 3C), reduced autophagy induction in ischemia (Figure 3D), and impaired survival in ischemia (Figure 3E). Similar results were obtained using RNAi targeting a different sequence in *beclin1* or another essential autophagy gene, *atg5* (Figure S2). Thus, autophagy enables survival of iBMK cells to metabolic stress when apoptosis is inactivated.

To address if autophagy is generally required for epithelial cancer cells to survive metabolic stress, HeLa cells were engineered with an apoptosis defect through BCL-x_L or BCL-2 expression, and Beclin1 was inhibited using RNAi. Knockdown of Beclin1 (Figure 3F) significantly reduced autophagy in metabolically stressed cells with (HeLa) or without (HeLa BCL-x_L or BCL-2) the capacity for apoptosis (Figure 3G). As in D3 cells, knockdown of Beclin1 reduced survival in HeLa cells expressing BCL-x_L or BCL-2 under ischemic conditions in comparison to the LaminA/C RNAi controls. In contrast, Beclin1 knockdown had no effect on the viability of HeLa cells with an intact apoptotic response

(Figure 3H). Therefore, the response of epithelial cancer cells to metabolic stress is apoptosis, which, when disabled by BAX/BAK deficiency or by BCL-x_L or BCL-2 expression, permits survival by autophagy. AKT activation, which inhibits autophagy (Arico et al., 2001) (Figure 2), or direct downregulation of Beclin1 blocks this survival pathway, stimulating necrotic cell death (Figure 3I). This reliance on autophagy for maintenance of cellular functions during metabolic stress may be further exacerbated by dependency on glycolytic metabolism conferred by AKT.

Necrosis is distinct from apoptosis and is a less efficient means of cell death

The data above illustrate that genetic determinants establish whether cells respond to metabolic stress with apoptosis, autophagy, or necrosis. To begin to compare the result of these three distinct responses to the same stimulus, multifield time-lapse microscopy was used to follow cell fates over 5 days in ischemia in vitro. W2 (Figures 4A and 4B) and W2 AKT (data not shown) underwent classic apoptosis between 24 and 72 hr characterized by an abrupt morphologic change (within 10 min) with membrane blebbing that was completed in under an hour. This is characteristic of apoptosis and consistent with the apoptotic nuclear morphology and caspase-3 activation (Figures 2A and 2B). Cell division in ischemia was limited to less than one prior to the onset of apoptosis (Figure 4A). In contrast, ischemia caused D3 AKT cells to undergo violent cytoplasmic vesicle movement (cytoplasmic boiling) and to become refractile and lyse within 48 hr by a process that was clearly distinguished from apoptosis (Figures 4A and 4B). Cell division in ischemic D3 AKT cells was rare, with less than 10% of the cell population dividing prior to the onset of necrosis (Figure 4A). Remarkably, D3 cells surviving ischemia by autophagy continued to proliferate for 72 hr, undergoing several cell divisions, after which proliferation and cell motility slowed to give way to progressive cellular condensation (condensation phase) culminating by 5 days (Figures 4A and 4B). However, following condensation, these condensed cells were not dead, as restoration of nutrients and oxygen results in reversal of this process and resumption of proliferation for the majority of cells (Figure 4A).

To compare the efficiency and extent of the different forms of cell death, W2, W2 AKT, D3, and D3 AKT cells were incubated under ischemic conditions for 3, 5, and 7 days, after which they were returned to normal growth conditions and evaluated for clonogenic survival. Both W2 and W2 AKT cells were killed rapidly and efficiently with survival of less than 1 in 10^6 cells following 5 days of ischemia, whereas D3 cells remained nearly completely viable even after 7 days in ischemia (Figure 4C). While D3 AKT cells displayed impaired clonogenic survival as expected, necrotic cell death was less efficient and much more asynchronous than apoptosis and resulted in gradual 10^2- to 10^3-fold impairment in clonogenic survival (Figure 4C).

Autophagy in tumors localizes to the center prior to acquisition of a blood supply

To determine when and where autophagy occurred during tumorigenesis, tumors generated from D3 cells stably expressing EGFP-LC3 were examined for membrane translocation at 1, 3, and 15 days following implantation in vivo. At days 1 (Figure 5A) and 3 (data not shown), EGFP-LC3 localization was diffuse only at the perimeter and was punctate, indicative of autophagy in the center of the tumor mass. Angiogenesis does not occur prior to day 3, and tumors are hypoxic, particularly in interior regions (Nelson et al., 2004). In contrast, at day 15, by which time D3 tumors have established a blood supply and are no longer hypoxic (Nelson et al., 2004), the localization of EGFP-LC3 was diffuse, with only scattered rare cells displaying punctate localization (Figure 5B). Thus, autophagy localizes to unvascularized, metabolic stressed regions of tumors. Further conformation of the spatial and temporal occurrence of autophagy in tumors awaits a similar analysis of the *beclin1*$^{+/+}$ and *beclin1*$^{+/-}$ tumors (see below).

Role of *beclin1* in oncogene-activated necrosis

To directly address the contribution of autophagy inhibition by AKT to induction of necrosis and stimulation of tumorigenesis, iBMK cells with allelic loss of the essential autophagy gene *beclin1* were generated and examined. All *beclin1*$^{+/-}$ and *beclin1*$^{+/+}$ iBMK cell lines expressed E1A and p53DD, and reduced Beclin1 expression was observed as expected in *beclin1*$^{+/-}$ cell lines (Figure 6A). *beclin1*$^{+/+}$ and *beclin1*$^{+/-}$ iBMK cells were engineered without and with an apoptosis defect (BCL-2 expression, Figure 6A) to document the impact of a reduced capacity for autophagy on survival and method of cell death.

Reduced constitutive autophagy was apparent in *beclin1*$^{+/-}$ cells (1%) compared to *beclin1*$^{+/+}$ cells (3.5%) even under normal growth conditions as measured by EGFP-LC3 translocation. As with W2 cells, ischemia efficiently induced autophagy in *beclin1*$^{+/+}$ cells prior to apoptosis (59% at 6 hr of ischemia), and allelic loss of *beclin1* impaired autophagy (18% at 6 hr of ischemia) without altering the time course of apoptosis (Figure 6D). BCL-2 expression blocked apoptosis (Figure 6D), and *beclin1* haploinsufficiency diminished constitutive autophagy and its induction in ischemia (Figures 6B and 6C). Autophagy induction levels in the BCL-2-expressing cells were robust and similar to BAK/BAK-deficient cells, suggesting that inhibition of Beclin1 by BCL-2 (Pattingre et al., 2005; Shimizu et al., 2004) is not a significant factor in these circumstances.

Multiple independent BCL-2-expressing *beclin1*$^{+/+}$ and *beclin1*$^{+/-}$ iBMK cell lines, and representative *beclin1*$^{+/+}$ and *beclin1*$^{+/-}$ cell lines without BCL-2, were incubated in ischemia, and viability was assessed. Both wild-type and *beclin1*$^{+/-}$ cells were readily killed over the course of 2 days as expected, whereas wild-type cells expressing BCL-2 were markedly resistant, with the number of viable cells increasing in the first 24 hr (Figure 6D). Little effect of *beclin1* haploinsufficiency was apparent in cells with an apoptotic response. In the background of an apoptosis defect, however, *beclin1* haploinsufficiency diminished the survival advantage provided by BCL-2 (Figure 6D). These findings are consistent with the restoration of cell death in ischemic D3 and HeLa BCL-x_L and BCL-2 cells, where Beclin1 and autophagy were compromised by RNAi (Figure 3).

To extend these observations, *beclin1*$^{+/+}$ and *beclin1*$^{+/-}$ iBMK cell lines expressing BCL-2 (WB-13 and BLNB-12, respectively) were examined over the course of 3 days by time-lapse microscopy. BCL-2 protected wild-type cells from cell death by ischemia (Figures 6D and 6E) similarly to D3 cells (Figures 4A and 4C), which otherwise show substantially reduced viability by 48 hr (Figures 2 and 4). BCL-2 expression in wild-type cells allowed 1 to 2 rounds of cell division in the first 24 hr in ischemia (Figures 6D and 6E). Cellular condensation commenced on day 2 and continued through day 3, with the majority of the cells retaining viability (Figures 6D and 6E). In contrast, the ability of BCL-2 to provide protection from ischemia was diminished in the *beclin1*$^{+/-}$ cells. Cell division in ischemic conditions was halted rapidly, with only one in five cells dividing in the first 24 hr, followed by cell death resembling necrosis (Figures 6D and 6E). EM revealed condensed but healthy morphology of *beclin1*$^{+/+}$ BCL-2 cells, but vacuolated and necrotic morphology of *beclin1*$^{+/-}$ BCL-2 cells by 7 days in ischemia (Figure 6F), indicative of failed organelle integrity (Figure 6F). Thus, in the background of a defect in apoptosis, autophagy can temporarily sustain homeostasis under conditions of metabolic stress. Cells that are defective for autophagy, however, lack this capacity to insulate themselves from fluctuations in external nutrient availability, which renders them vulnerable to metabolic stress.

Autophagy deficiency promotes tumor growth and necrosis

Haploinsufficiency in *beclin1* impairs autophagy and promotes tumorigenesis in mice, and *beclin1* is monoallelically deleted in many breast, prostate, and ovarian tumors, indicating a

role for autophagy in tumor suppression (Edinger and Thompson, 2003; Liang et al., 1999; Qu et al., 2003; Yue et al., 2003). Disabling both apoptosis and autophagy in stressed cells may be a formula for induction of necrotic cell death, but whether this is related to the mechanism by which *beclin1* haploinsufficiency promotes tumorigenesis is not known. To test the roles of defective apoptosis and autophagy on tumorigenesis, *beclin1*$^{+/+}$ and *beclin1*$^{+/-}$ iBMK cells without and with BCL-2 were evaluated for tumor growth. *beclin1*$^{+/+}$ iBMK cells formed tumors only with prolonged latency (greater than 2 months) (Figure 7A) as expected and consistent with clonal emergence (Degenhardt et al., 2002a; Nelson et al., 2004; Tan et al., 2005). Allelic loss of *beclin1* slightly accelerated tumor growth compared to *beclin1*$^{+/+}$ cells, but tumor growth still took 2 months (Figure 7A), consistent with a modest increase in the frequency of clonal emergence. BCL-2 accelerated tumor growth, which was accelerated even further by allelic loss of *beclin1* (Figure 7B). Thus, defective autophagy stimulates tumor growth and synergizes with defective apoptosis to promote tumorigenesis. *beclin1*$^{+/-}$ BCL-2 tumor growth was still substantially slower than that of the D3 AKT tumors (Figure 1B), suggesting that inhibition of autophagy by AKT contributes to tumorigenesis but that other AKT functions also play a role in promoting tumor growth. Finally, tumor histology revealed a greater prevalence of necrosis in BCL-2-expressing *beclin1*$^{+/-}$ compared to *beclin1*$^{+/+}$ tumors (Figure 7C), consistent with the possibility that altering the mode of cell death from apoptosis or autophagy to necrosis can impact tumor growth. Beclin1 haploinsufficient tumors, however, were not as necrotic as tumors with activated AKT, indicating that altered metabolism or growth conferred by AKT may further promote necrosis.

Tumor necrosis stimulates an inflammatory response

Oncogene-activated necrosis in vivo is associated with enhanced tumor growth. To begin to address the possibility that there is a differential immune response to nonnecrotic and necrotic tumors that may influence tumor growth, D3 and D3 AKT tumors were evaluated for evidence of macrophage infiltration (Mac3 IHC). D3 tumors showed few macrophages, whereas the D3 AKT tumors displayed massive macrophage infiltration throughout all necrotic areas up to the border of healthy tumor tissue (Figure 8A); thus, tumor necrosis is associated with macrophage infiltration. Macrophages and other cells constituting an inflammatory infiltrate produce cytokines and chemokines that impact cell proliferation, angiogenesis, and recruitment of other immune effector cells to the site of a wound, infection, or tumor. Indeed, strong p50 NF-κB IHC staining (both nuclear and cytoplasmic) was observed throughout D3 AKT healthy tumor tissue that was less apparent in D3 tumors (Figure 8B). Furthermore, higher activity of the cytokine and NF-κB-responsive IL-6 promoter-LUC reporter was observed in D3 AKT tumors compared to D3 tumors in vivo (Figure 8C). Thus, oncogene-activated tumor necrosis stimulates the innate immune response that has the potential to impact tumor growth (Figure 8D).

Discussion

Metabolic stress is a common occurrence in human tumors that can potently induce cell death by apoptosis; however, in tumor cells possessing an apoptotic defect this results instead in induction of autophagy, which supports survival. Catabolism and elimination of damaged organelles by autophagy may serve to maintain normal cellular function under conditions of fluctuating oxygen and nutrient supply. Autophagy may thereby be beneficial as a buffer to short-term interruptions in nutrient availability.

The PI3-kinase/AKT pathway stimulates cell growth in response to nutrients in part through activating mTOR, which promotes protein synthesis while inhibiting autophagy (Guertin and Sabatini, 2005). Constitutive activation of this PI3-kinase/AKT/mTOR signaling may render cells susceptible to metabolic catastrophe upon nutrient limitation by increasing

energy demand and promoting inefficient energy production (glycolysis) while curtailing the ability to use autophagy. Constitutive activation of AKT is a common event in oncogenesis that deregulates cell growth and uncouples nutrient availability from proper downregulation of metabolism. The combined inactivation of apoptosis and activation of AKT results in induction of necrotic cell death under starvation conditions, demonstrating a level of genetic control governing the propensity for necrosis.

Association of necrosis, inflammation, and tumorigenesis

In tumors, as is the case for physical injury, necrosis is associated with inflammation. With physical injury, inflammation is part of wound healing, where cellular infiltration and chemokine and cytokine production function to stimulate proliferation, tissue remodeling, and angiogenesis to facilitate repair. The inflammatory response to stress-mediated, oncogene-activated necrosis in tumors, by analogy to a wound healing response, may stimulate angiogenesis and tumor cell proliferation (Balkwill et al., 2005; Balkwill and Coussens, 2004; Vakkila and Lotze, 2004; Zeh and Lotze, 2005). Local activation of an innate immune response in tumors in the absence of T cells as described here may serve to promote tumor progression but may facilitate tumor regression by recruiting a T cell response. However, recent evidence also suggests that tumor-associated inflammation can enhance tumor progression in an immune competent host (Balkwill and Coussens, 2004; Greten et al., 2004; Pikarsky et al., 2004). How inflammation alters the tumor microenvironment and modulates tumorigenesis requires further investigation.

Apoptosis may be the preferred means of cell death for epithelial cells upon damage or stress, as cell elimination occurs without inflammation. If apoptosis fails, autophagy can sustain viability in the short term and possibly lead to cell death in the long term without inflammation. Inhibition of autophagy in tumors with a defective apoptotic response under conditions of metabolic stress is an effective means of diverting normally death-refractory cells to an alternate necrotic cell death pathway. This suggests that apoptosis and autophagy function to limit necrosis. Thus, autophagy may be therapeutically targeted for tumors with defects in apoptosis; however, stimulation of necrosis and activation of an inflammatory response may impact tumor growth. Alternatively, exploitation of autophagy as a means to cell death selectively in tumor cells represents another attractive therapeutic strategy.

Genetic determinants of necrosis

Activation of necrotic cell death in apoptosis-defective epithelial cells by AKT and ischemia demonstrates a link between the cell's metabolic state, stress responses, and the function of BCL-2 family members. This suggests that necrotic cell death can be genetically determined, oncogene activated, and triggered by an inability to adapt to metabolic stress. Indeed, PARP deficiency mitigates necrotic cell death by delaying ATP consumption in response to alkylating agents (Zong et al., 2004). Although the BCL-2 family is known for apoptosis regulation, our evidence suggests that by blocking apoptosis they also may delay necrosis by allowing autophagy. Cells can thereby undergo apoptosis, necrosis, or autophagy depending on their genetic makeup and the physiological conditions. This may be important for preventing inflammation by implementing apoptosis, and essential for surviving periods of intermittent nutrient limitation through autophagy, but may facilitate wound healing in the case of necrosis. Thus, necrosis may be a regulated process functionally interdependent on apoptosis and autophagy.

Establishing the genetic determinants regulating necrotic cell death is likely to be essential for successful cancer treatment (Nelson and White, 2004) and preventing degenerative diseases (Driscoll and Gerstbrein, 2003). Indeed, the metabolic state of tumor cells, specifically stimulation of aerobic glycolysis by AKT (Elstrom et al., 2004), promotes

necrotic cell death in response to DNA alkylating agents that may be the basis for their successful use in chemotherapy regimens (Zong et al., 2004). Exploitation of the altered metabolic state of tumors (Warburg, 1956) either through the dependency on glycolysis or autophagy may be therapeutically advantageous.

Autophagy allows temporary survival to metabolic stress

beclin1 haploinsufficiency promotes tumorigenesis in mice and is found with high frequency in human breast, ovarian, and prostate cancers (Liang et al., 1999; Qu et al., 2003; Yue et al., 2003); however, the molecular basis by which a reduced capacity for autophagy promotes tumorigenesis is unknown. Our data suggest that *beclin1* haploinsufficiency may have the largest impact on cells that also possess an apoptotic defect, which prevents an apoptotic response to starvation, allowing survival by autophagy. One striking observation was the initial uninterrupted proliferation of the BAX/BAK-deficient or BCL-2-expressing iBMK cells in ischemia (Figures 4A, 6D, and 6E). This was contrasted by cessation of cell division, failure of organelle integrity, and facilitation of necrosis in the apoptosis-defective cells with either activated AKT or allelic loss of *beclin1* where autophagy was compromised. This suggests that defective apoptosis reveals the capacity for autophagy to temporarily sustain normal cell function in situations of fluctuating nutrient availability. Autophagy may thereby mitigate the potentially damaging impact of repetitious cycles of metabolic stress as a tumor suppression mechanism.

Impact of deficient autophagy on tumorigenesis

The ability of allelic loss of *beclin1* to cooperate with RB, p53, and apoptosis defects to promote tumorigenesis (Figure 7B) suggests that deficient autophagy functions in a separate pathway. This is consistent with autophagy being downstream of mTOR, and with the loss of autophagy contributing to the tumor-promoting activity of AKT. It is important to consider that the failure of tumor cells to buffer metabolic stress may promote tumorigenesis in multiple ways, of which preventing cellular damage and altering the tumor microenvironment by promoting necrosis may only be part of the mechanism. It will be interesting to determine if allelic loss of *beclin1* increases genomic instability induced by metabolic stress in cells with a defect in apoptosis (Nelson et al., 2004). Alternatively, prolonged metabolic stress may lead to autophagic cell death as a tumor suppression mechanism, the failure of which may promote tumorigenesis through enhanced survival of damaged cells.

Experimental procedures

Generation of cell lines

To obtain independent *beclin1*$^{+/+}$ and *beclin1*$^{+/-}$ iBMK cell lines, *beclin1*$^{+/-}$ mice were intercrossed, and primary kidney epithelial cells from 5-day-old pups were immortalized by E1A and dominant-negative p53 (p53DD) expression and propagated and genotyped as previously described (Degenhardt et al., 2002b; Yue et al., 2003). iBMK cells expressing human BCL-2, H-ras, RAF-CAAX, *myr*-AKT, and the vector controls were derived by electroporation with pcDNA3.1-hBCL-2 (Kasof et al., 1998), pcDNA1.H-rasV12 (Lin et al., 1995), pcDNA3.RAF-CAAX (provided by Dr. Peter Sabbatini, UCSF, San Francisco, CA), pcDNA3.Myr-AKT (Plas et al., 2001), or vector (W2, pcDNA3.1; D3, pcDNA3.1zeo, Invitrogen, Carlsbad, CA), followed by selection (W2, geneticin; D3, zeocin). Tumor formation by subcutaneous injection in nude mice was described previously (Degenhardt et al., 2002a) (see Supplemental Data). HeLa cells and those expressing human BCL-x_L or BCL-2 were derived by electroporation with vector (pcDNA3.1, Invitrogen), pcDNA3.1-h-BCL-x_L (Han et al., 1998), or pcDNA3.1-hBCL-2 (Kasof et al., 1998), respectively, followed by selection with geneticin and verification of protein expression and function.

Western blotting, IHC, immunofluorescence, and EM

The following antibodies were used: anti-Beclin1 (Santa Cruz, Santa Cruz, CA); anti-ATG5 (Mizushima et al., 2001); anti-BAX and -BAK (Upstate Biotechnology, Lake Placid, NY); anti-BCL-2 (Santa Cruz); anti-p53 (Ab-1); anti-E1A and -actin (Oncogene, Cambridge, MA); anti-HMGB1 (ABCAM, Cambridge, MA); anti-p50 (Santa Cruz); and anti-Mac3 (BD Pharmingen). Western blotting and IHC were performed as previously described (Nelson et al., 2004). Cells were examined by EM using a JEOL 1200EX electron microscope.

In vitro ischemia

Cells were placed in glucose-free DMEM (Invitrogen) containing 10% FBS and incubated with a defined gas mixture containing 1% oxygen, 5% CO_2, and 94% N_2 (AirGas, Piscataway, NJ) (Nelson et al., 2004). Viability was assessed by trypan blue exclusion, and EGFP-LC3 translocation was quantitated by determining the number of transfected cells displaying any indication of punctate (rather than diffuse) fluorescence out of a population of 300 cells. Determination of DNA content by FACS analysis of propidium iodide-stained cells was performed using a Cytomics FC 500 (Beckman Coulter). Multifield time-lapse was performed as described in the Supplemental Data.

RNA interference

Cells were transfected with annealed, purified, and desalted double-stranded siRNA (30 μg/3×10^6 cells) using the Amaxa nucleofection system (kit V, program G-16). siRNA targeted against *beclin1* (5′-AACUUGCUUUACUCUCUCUAUCA-3′) (Shimizu et al., 2004) (Figure S2) or (5′-CAGUUUGGCACAAUCAAUAUU-3′) (Hoyer-Hansen et al., 2005) (Figure 3), murine *atg5* (5′-AAGAUCCUGGACCGGUCACC-3′) (Shimizu et al., 2004), and *LaminA/C* were obtained from Dharmacon Research (Lafayette, CO).

In vivo luciferase reporter assays

Tumors were monitored for in vivo promoter activation by using an IVIS in vivo luminescence imaging System (Xenogen Corp., Alameda, CA) by intraperitoneal injection with D-luciferin potassium salt (Xenogen Corp.) approximately 15 min prior to imaging using an IACUC-approved protocol. Luminescence bio-photonic quantitation (photons/cm^2/s) was analyzed using Living Image Software (Xenogen Corp.). The total photon values were normalized to basal luminescence activity at day 2 postinjection and compared to that after tumor growth where tumor sizes were comparable.

SIGNIFICANCE

While the role of apoptosis in tumor suppression is well known, the importance of other forms of cell death, autophagy and necrosis, is only recently becoming realized. Autophagy is a catabolic process initiated by starvation, whereby cells self-digest intracellular organelles as a mechanism of cell survival or cell death. Mice with an allelic loss of the essential autophagy regulator *beclin1* are tumor prone, although the mechanism involved is not known. Alternatively, necrosis results in cell lysis and in cancer is associated with poor prognosis. We show that autophagy promotes cell survival in solid tumors and that coordinate inactivation of apoptosis and autophagy promotes necrosis and tumor progression associated with inflammation.

Supplementary Material

Refer to Web version on PubMed Central for supplementary material.

Acknowledgments

We thank Thomasina Sharkey for assistance with preparation of the manuscript. This work was supported by a grant from the National Institutes of Health (R37 CA53370) to E.W. and the Howard Hughes Medical Institute. We thank Raj Patel for assistance with the EM and Drs. Plas, Sabbatini, and Mizushima for providing reagents.

References

Adams JM. Ways of dying: multiple pathways to apoptosis. Genes Dev 2003;17:2481–2495. [PubMed: 14561771]

Arico S, Petiot A, Bauvy C, Dubbelhuis PF, Meijer AJ, Codogno P, Ogier-Denis E. The tumor suppressor PTEN positively regulates macroautophagy by inhibiting the phosphatidylinositol 3-kinase/protein kinase B pathway. J Biol Chem 2001;276:35243–35246. [PubMed: 11477064]

Balkwill F, Coussens LM. Cancer: An inflammatory link. Nature 2004;431:405–406. [PubMed: 15385993]

Balkwill F, Charles KA, Mantovani A. Smoldering and polarized inflammation in the initiation and promotion of malignant disease. Cancer Cell 2005;7:211–217. [PubMed: 15766659]

Danial NN, Korsmeyer SJ. Cell death: Critical control points. Cell 2004;116:205–219. [PubMed: 14744432]

Degenhardt K, Chen G, Lindsten T, White E. Bax and Bak mediate p53-independent suppression of tumorigenesis. Cancer Cell 2002a;2:193–203. [PubMed: 12242152]

Degenhardt K, Sundararajan R, Lindsten T, Thompson CB, White E. Bax and Bak independently promote cytochrome-c release from mitochondria. J Biol Chem 2002b;277:14127–14134. [PubMed: 11836241]

Driscoll M, Gerstbrein B. Dying for a cause: invertebrate genetics takes on human neurodegeneration. Nat Rev Genet 2003;4:181–194. [PubMed: 12610523]

Edinger AL, Thompson CB. Defective autophagy leads to cancer. Cancer Cell 2003;4:422–424. [PubMed: 14706333]

Elstrom RL, Bauer DE, Buzzai M, Karnauskas R, Harris MH, Plas DR, Zhuang H, Cinalli RM, Alavi A, Rudin CM, Thompson CB. Akt stimulates aerobic glycolysis in cancer cells. Cancer Res 2004;64:3892–3899. [PubMed: 15172999]

Gottlob K, Majewski N, Kennedy S, Kandel E, Robey RB, Hay N. Inhibition of early apoptotic events by akt/PKB is dependent on the first committed step of glycolysis and mitochondrial hexokinase. Genes Dev 2001;15:1406–1418. [PubMed: 11390360]

Greten FR, Echmann L, Greten TF, Park JM, Li ZW, Egan LJ, Kagnoff MF, Karin M. IKKβ links inflammation and tumorigenesis in a mouse model of colitis-associated cancer. Cell 2004;118:285–296. [PubMed: 15294155]

Guertin DA, Sabatini DM. An expanding role for mTOR in cancer. Trends Mol Med 2005;11:353–361. [PubMed: 16002336]

Han J, Modha D, White E. Interaction of E1B 19K with Bax is required to block Bax-induced loss of mitochondrial membrane potential and apoptosis. Oncogene 1998;17:2993–3005. [PubMed: 9881701]

Hanada M, Feng J, Hemmings BA. Structure, regulation and function of PKB/AKT—a major therapeutic target. Biochim Biophys Acta 2004;1697:3–16. [PubMed: 15023346]

Hoyer-Hansen M, Bastholm L, Mathiasen IS, Elling F, Jaattela M. Vitamin D analog EB1089 triggers dramatic lysosomal changes and Beclin 1-mediated autophagic cell death. Cell Death Differ 2005;12:1297–1309. [PubMed: 15905882]

Kamatsu M, Waguri S, Ueno T, Iwata J, Murato S, Tanida I, Ezaki J, Mizushima N, Ohsumi Y, Uchiyama Y, et al. Impairment of starvation-induced and constitutive autophagy in Atg7-deficient mice. J Cell Biol 2005;169:425–434. [PubMed: 15866887]

Kanduc D, Mittelman A, Serpico R, Sinigaglia E, Sinha AA, Natale C, Santacroce R, DiCorcia MG, Lucchese A, Dini L. Cell death: Apoptosis versus necrosis. Int J Oncol 2002;21:165–170. [PubMed: 12063564]

Karnauskas R, Niu Q, Talapatra S, Plas DR, Greene ME, Crispino JD, Rudin CM. Bcl-x_L and Akt cooperate to promote leukemogenesis *in vivo*. Oncogene 2003;22:688–698. [PubMed: 12569361]

Kasof GM, Rao L, White E. Btf: A novel death-promoting transcriptional repressor that interacts with Bcl-2 related proteins. Mol Cell Biol 1998;19:4390–4404. [PubMed: 10330179]

Kuma A, Hatano M, Matsui M, Yamamoto A, Nakaya H, Yoshimori T, Ohsumi Y, Tokuhisa T, Mizushima N. The role of autophagy during the early neonatal starvation period. Nature 2004;432:1032–1036. [PubMed: 15525940]

Levine B. Eating oneself and uninvited guests: Autophagy-related pathways in cellular defense. Cell 2005;120:159–162. [PubMed: 15680321]

Liang XH, Jackson S, Seaman M, Brown K, Kempkes B, Hibshoosh H, Levine B. Induction of autophagy and inhibition of tumorigenesis by beclin 1. Nature 1999;402:672–676. [PubMed: 10604474]

Lin HJL, Eivner V, Prendergast GC, White E. Activated H-ras rescues E1A-induced apoptosis and cooperates with E1A to overcome p53-dependent growth arrest. Mol Cell Biol 1995;15:4536–4544. [PubMed: 7623844]

Majno G, Joris I. Apoptosis, oncosis, and necrosis. An overview of cell death. Am J Pathol 1995;146:3–15. [PubMed: 7856735]

Mizushima N, Yamamoto A, Hatano M, Kobayashi Y, Kabeya Y, Suzuki K, Tokuhisa T, Ohsumi Y, Yoshimori T. Dissection of autophagosome formation using Apg5-deficient mouse embryonic stem cells. J Cell Biol 2001;152:657–668. [PubMed: 11266458]

Mizushima N, Yamamoto A, Matsui M, Yoshimori T, Ohsumi Y. In vivo analysis of autophagy in response to nutrient starvation using transgenic mice expressing a fluorescent autophagosome marker. Mol Biol Cell 2004;15:1101–1111. [PubMed: 14699058]

Nelson D, White E. Exploiting different ways to die. Genes Dev 2004;18:1223–1226. [PubMed: 15175258]

Nelson D, Tan TT, Rabson AB, Anderson D, Degenhardt K, White E. Hypoxia and defective apoptosis drive genomic instability and tumorigenesis. Genes Dev 2004;18:2095–2107. [PubMed: 15314031]

Pattingre S, Tassa A, Qu X, Garuti R, Liang XH, Mizushima N, Packer M, Schneider MD, Levine B. Bcl-2 antiapoptotic proteins inhibit beclin 1-dependent autophagy. Cell 2005;122:927–939. [PubMed: 16179260]

Pikarsky E, Porat RM, Stein I, Abramovitch R, Amit S, Kasem S, Gutkovich-Pyest E, Urieli-Shoval S, Galun E, Ben-Neriah Y. NF-κB functions as a tumour promoter in inflammation-associated cancer. Nature 2004;431:461–466. [PubMed: 15329734]

Plas DR, Talapatra S, Edinger AL, Rathmell JC, Thompson CB. Akt and Bcl-x_L promote growth factor-independent survival through distinct effects on mitochondrial physiology. J Biol Chem 2001;276:12041–12048. [PubMed: 11278698]

Proskuryakov SY, Konoplyannikov AG. Necrosis: a specific form of programmed cell death? Exp Cell Res 2003;283:1–16. [PubMed: 12565815]

Qu X, Yu J, Bhagat G, Furuya N, Hibshoosh H, Troxel A, Rosen J, Eskelinen EL, Mizushima N, Ohsumi Y, et al. Promotion of tumorigenesis by heterozygous disruption of the beclin 1 autophagy gene. J Clin Invest 2003;112:1809–1820. [PubMed: 14638851]

Scaffidi P, Misteli T, Bianchi ME. Release of chromatin protein HMGB1 by necrotic cells triggers inflammation. Nature 2002;418:191–195. [PubMed: 12110890]

Shimizu S, Kanaseki T, Mizushima N, Mizuta T, Arakawa-Kobayashi S, Thompson CB, Tsujimoto Y. Role of Bcl-2 family proteins in a non-apoptotic programmed cell death dependent on autophagy genes. Nat Cell Biol 2004;6:1221–1228. [PubMed: 15558033]

Tan TT, Degenhardt K, Nelson DA, Beaudoin B, Nieves-Neira W, Bouillet P, Villunger A, Adams JM, White E. Key roles of BIM-driven apoptosis in epithelial tumors and rational chemotherapy. Cancer Cell 2005;7:227–238. [PubMed: 15766661]

Tanida I, Ueno T, Kominami E. LC3 conjugation system in mammalian autophagy. Int J Biochem Cell Biol 2004;36:2503–2518. [PubMed: 15325588]

Vakkila J, Lotze MT. Inflammation and necrosis promote tumour growth. Nat Rev Immunol 2004;4:641–648. [PubMed: 15286730]

Warburg O. On respiratory impairment in cancer cells. Science 1956;124:269–270. [PubMed: 13351639]

Yue Z, Jin S, Yang C, Levine AJ, Heintz N. Beclin 1, an autophagy gene essential for early embryonic development, is a haploinsufficient tumor suppressor. Proc Natl Acad Sci USA 2003;100:15077–15082. [PubMed: 14657337]

Zeh HJI, Lotze MT. Addicted to death. J Immunother 2005;28:1–9. [PubMed: 15614039]

Zong WX, Thompson CB. Necrotic death as a cell fate. Genes Dev 2006;20:1–15. [PubMed: 16391229]

Zong WX, Ditsworth D, Bauer DE, Wang ZQ, Thompson CB. Alkylating DNA damage stimulates a regulated form of necrotic cell death. Genes Dev 2004;18:1272–1282. [PubMed: 15145826]

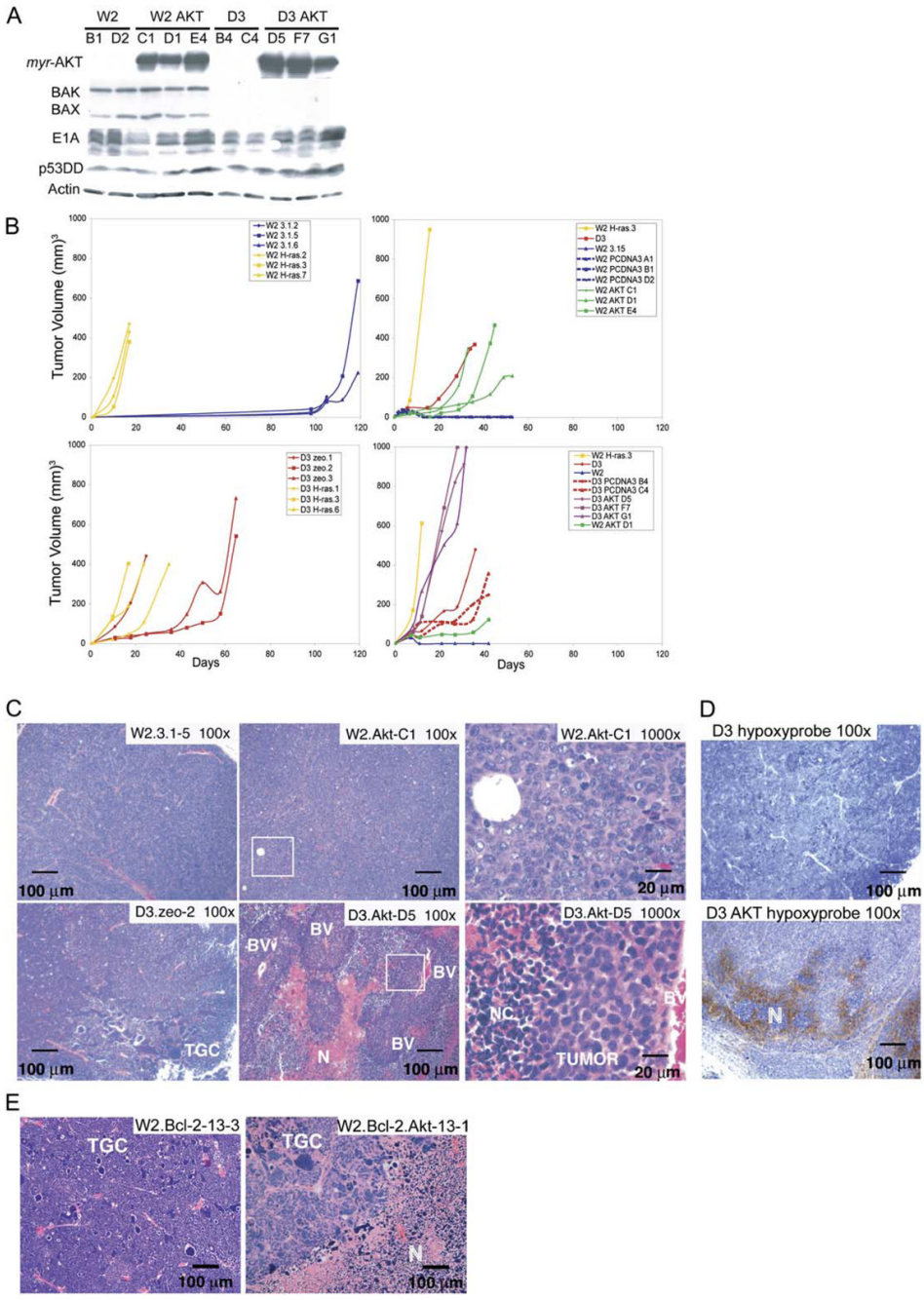

Figure 1. AKT and RAS promote tumor growth in both wild-type and apoptosis-defective genetic backgrounds

A: Western blots showing protein expression in the W2 and D3 derived vector control and AKT-expressing iBMK cell lines.

B: Tumor growth kinetics of iBMK cell lines. W2 vector controls (blue) compared to W2 derivatives expressing RAS (yellow). W2 vector control (blue) compared to W2 derivatives expressing *myr*-AKT (green). BAX/BAK-deficient D3 (red) and W2 plus RAS (yellow) are included for comparison. Addition of RAS to BAX/BAK-deficient D3 cells accelerates tumor growth as depicted by D3 (red) and D3 plus RAS (yellow). AKT promotes tumor growth of apoptosis-defective D3 cells as depicted by D3 AKT cells (purple). W2 (blue),

W2 plus AKT (green), D3 and D3 vector controls (red), and W2 plus RAS (yellow) are shown for comparison.

C: H&E staining of W2, W2 AKT, D3, and D3 AKT tumors illustrating tumor giant cells (TGC), necrosis (N), necrotic cells (NC), blood vessels (BV), and healthy tumor (TUMOR). Boxes indicate location of magnified areas.

D: Hypoxyprobe staining (Nelson et al., 2004) of D3 AKT and D3 tumors indicating hypoxic conditions associated with necrotic regions in D3 AKT tumors.

E: H&E staining of W2 BCL-2 tumors and W2 BCL-2 AKT tumors (Nelson et al., 2004) illustrating the pronounced necrosis (N) induced by AKT activation independent of the means of apoptosis inhibition.

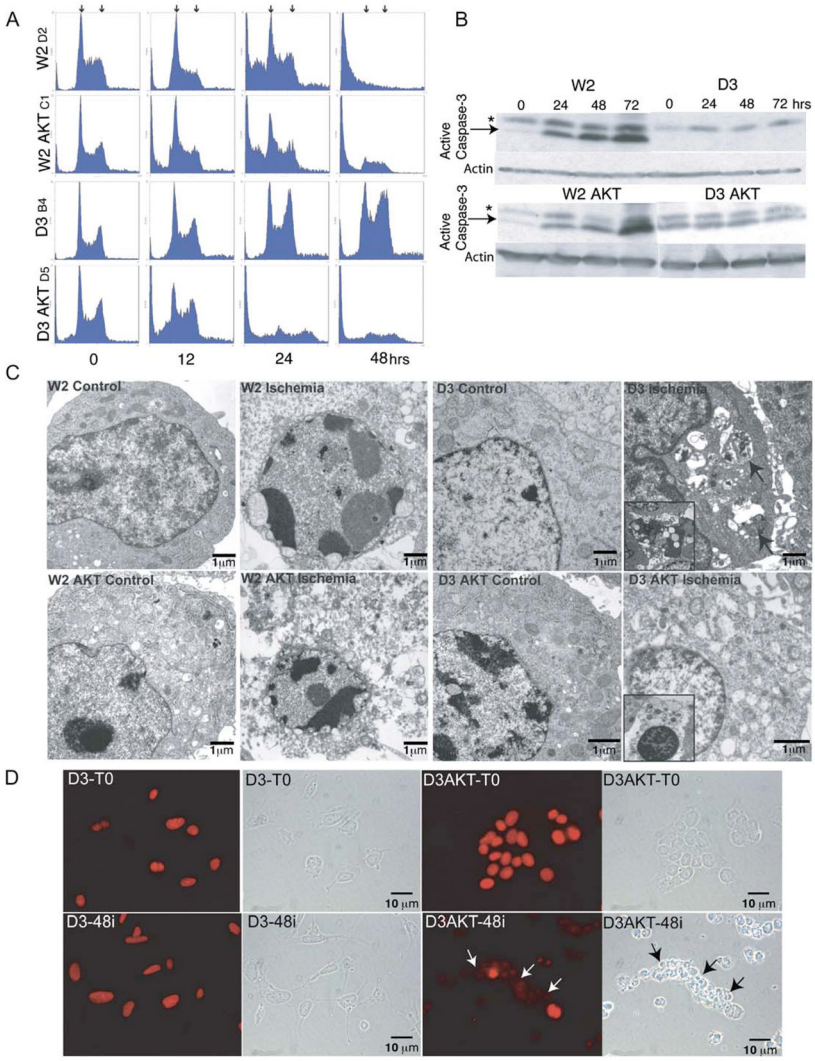

Figure 2. Ischemia induces autophagy in BAX/BAK-deficient iBMK cells that is diverted to necrosis by AKT activation

A: Flow cytometry of W2, W2 AKT, D3, and D3 AKT cells treated with ischemia in vitro for the indicated number of hours. Arrows indicate the positions of 2N/G1 (left) and 4N/G2/M (right) DNA content.

B: Induction of caspase-3 activation in W2 and W2 AKT but not in D3 or D3 AKT cells in response to ischemia in vitro. Western blot of cell extracts indicates p17 active caspase-3 band (arrows) and nonspecific band (*).

C: EM of untreated and ischemic (48 hr) W2, W2 AKT, D3, and D3 AKT cells from **A**. Note the apoptotic morphology of W2 and W2 AKT cells, the autophagy morphology of D3 cells (arrows indicate membranous organelle-like accumulations within vacuoles), and the necrotic morphology with vacuolated cytoplasm of D3 AKT cells. Insets represent progressive and distinctive endpoints indicative of autophagy (D3), or necrosis displaying a completely condensed nucleus (D3 AKT).

D: Loss of nuclear HMGB1 staining in necrotic D3 AKT (arrows) but not D3 cells in ischemia (48 hr) as a marker of necrosis.

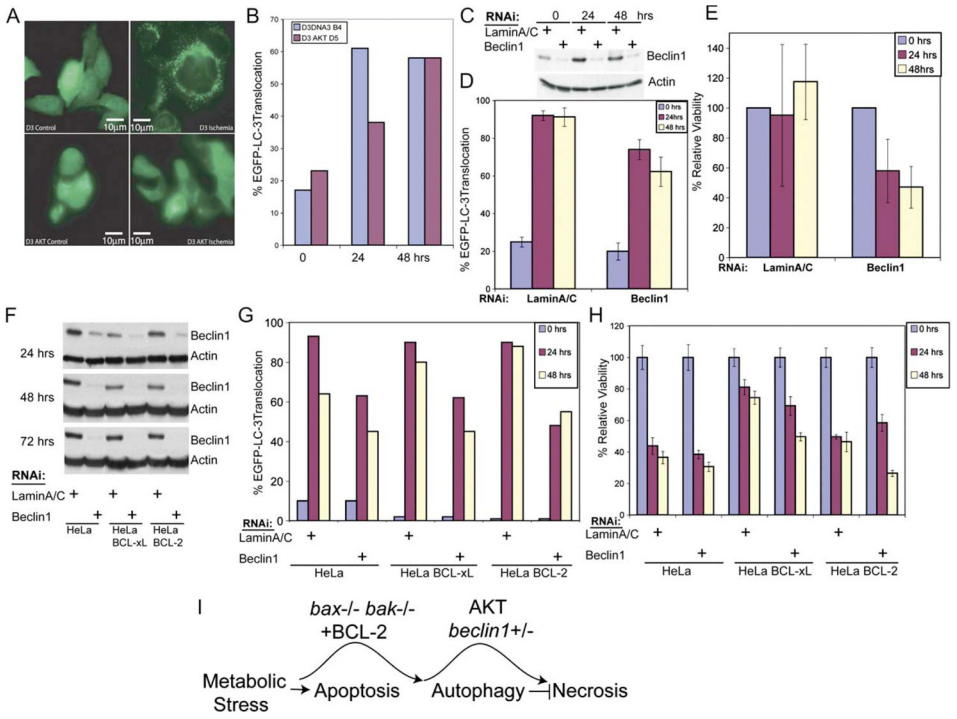

Figure 3. Ischemia induces autophagy in apoptosis-defective cells that when inhibited by AKT promotes cell death by necrosis

A: BAX/BAK-deficient D3 cells without and with AKT expressing the autophagy marker EGFP-LC3 were untreated or placed under ischemic conditions for 24 hr. EGFP-LC3 displayed diffuse intracellular localization under normal growth conditions, and membrane translocation (punctate localization) indicative of autophagy was observed in ischemic D3 cells, which was substantially inhibited in D3 AKT cells.

B: Quantitation of EGFP-LC3 translocation in untreated and ischemic D3 and D3 AKT cells (representative of three independent experiments). Note that, although the D3 AKT cells treated with ischemia have a high proportion of cells with translocated LC3 by 2 days in ischemia, viability is low.

C: Western blot showing knockdown of Beclin1 in D3 cells relative to the LaminA/C control at 24, 48, and 72 hr posttransfection under normal culture conditions; hours posttransfection correspond to 0, 24, and 48 hr of ischemia in **D** and **E**.

D: Reduction of autophagy in D3 cells by Beclin1 RNAi from **C** assessed by EGFP-LC3 translocation.

E: Knockdown of Beclin1 impairs survival of D3 cells to metabolic stress. Viability of D3 cells from **C** and **D** was assessed at 0, 24, and 48 hr of ischemia.

F: Western blot time course of Beclin1 knockdown by RNAi relative to the LaminA/C control under normal culture conditions in HeLa vector control cells and HeLa cells expressing BCL-x_L or BCL-2.

G: Knockdown of Beclin1 in HeLa cells impairs autophagy induction by ischemia. Quantitation of EGFP-LC3 translocation in untreated (0 hr) and ischemic treated (24 and 48 hr) HeLa vector controls or HeLa cells expressing BCL-x_L or BCL-2 following Beclin1 or LaminA/C knockdown for 24 hr by RNAi.

H: Knockdown of Beclin1 in HeLa cells expressing BCL-x_L or BCL-2 under ischemic conditions induces cell death. Viability of HeLa cells without or with BCL-x_L or BCL-2 in response to ischemia with or without knockdown of Beclin1 by RNAi is described in **E** and **F**.

I: Model for functional ordering and regulation of death pathways leading to necrosis.
Values represent the mean ± standard deviation for n ≥ 3.
Error bars represent ± one standard deviation.

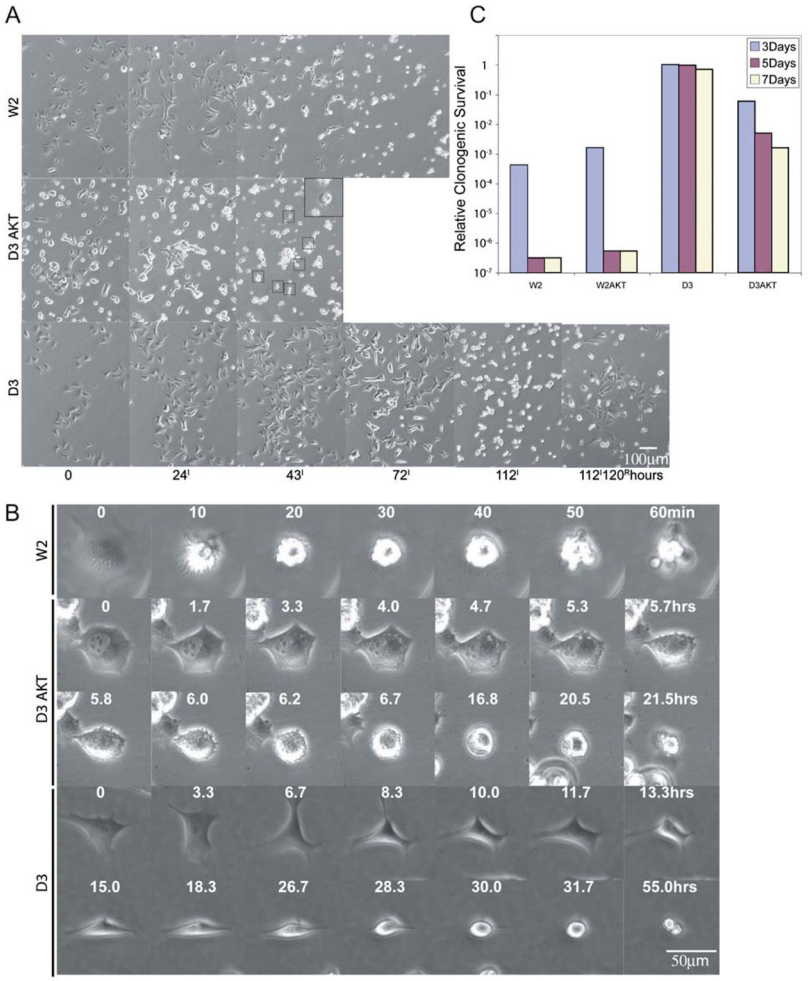

Figure 4. Distinct morphological features of apoptosis, necrosis, and autophagy in ischemia

A: Identical frames from 5 day time-lapse videos of the indicated cell lines in ischemia (100×). No morphological changes were apparent in W2 or D3AKT cells beyond 72 and 48 hr, respectively (data not shown). Boxed cells and inset (enlarged) show D3 AKT cells undergoing lysis. At 112 hr of ischemia, D3 cells were returned to normal culture conditions and photographed 120 hr later to document recovery. A representative frame of the recovery of D3 cells is shown.

B: Representative individual cells from **A** were followed for the indicated times beginning immediately prior to any signs of altered morphology in ischemia beginning at 13.5 hr for W2, 16.6 hr for D3 AKT, and 52.6 hr for D3.

C: Impact of different modes of cell death on clonogenic survival. W2, W2 AKT, D3, and D3 AKT cells were treated with ischemia for 3, 5, and 7 days, and the potential for clonogenic growth was determined following return to normal growth conditions (one of two replicates).

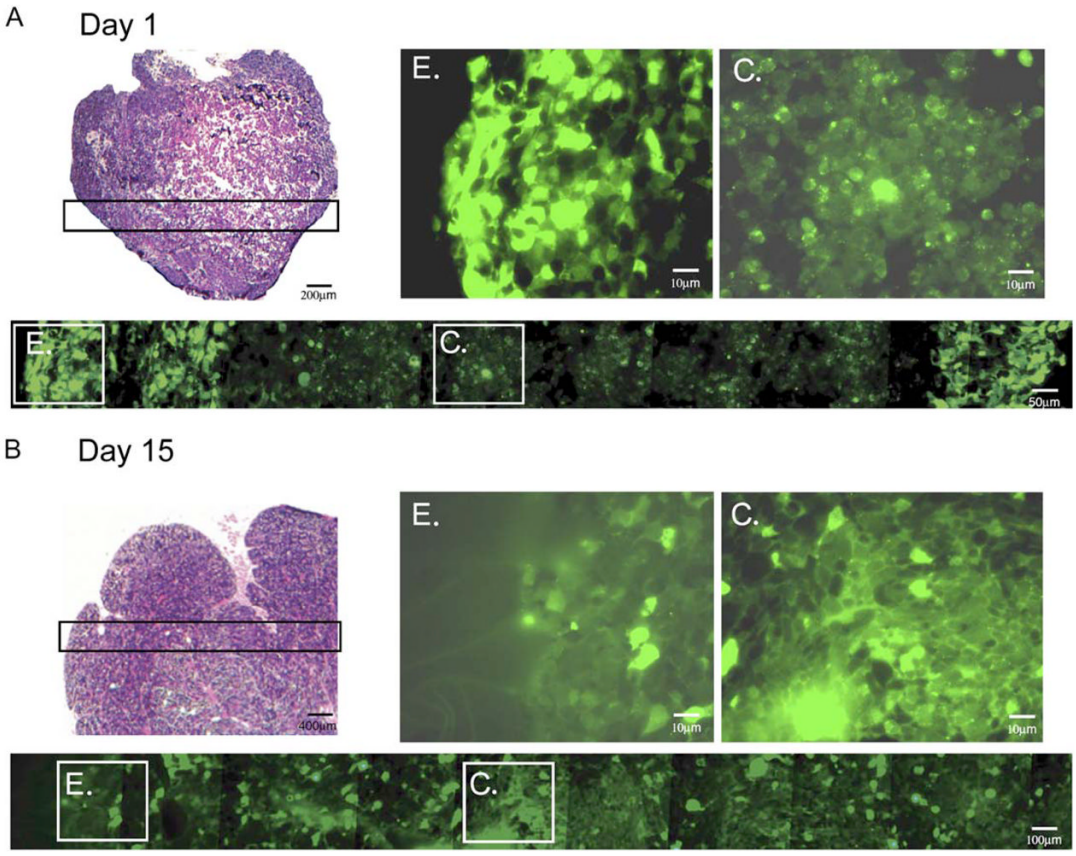

Figure 5. Autophagy in tumors localizes to regions of metabolic stress prior to angiogenesis

Tumors were established from D3 cells stably expressing EGFP-LC3 and monitored for membrane translocation indicative of autophagy at days 1 (**A**) and 15 (**B**) following implantation. Following excision, tumors were processed for histology (frozen sections) to preserve EGFP-LC3 fluorescence (Mizushima et al., 2004); a section through the entire tumor at day 1 and 1/4 of the tumor at day 15 is shown by H&E (magnification 40×), and a panorama across the tumor is shown for fluorescence (magnification 600×), as indicated. "E" and "C" indicate individual images from the tumor edge and center, respectively, enlarged to highlight the differential localization of EGFP-LC3 at day 1 that is diffuse at the tumor periphery and punctate in the center. Due to the compactness of the cells in the tumor, punctations may represent more than one autophagosome. Day 15 tumors have recruited a blood supply and display diffuse EGFP-LC3 localization throughout the tumor.

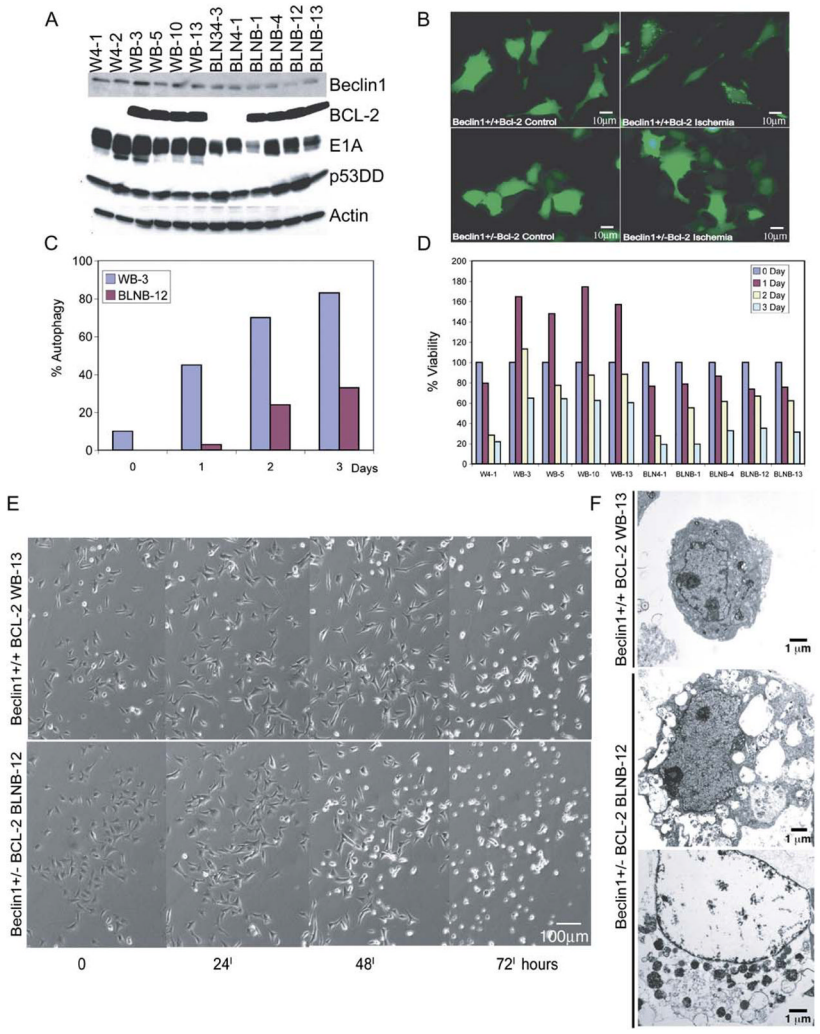

Figure 6. *beclin1* haploinsufficiency impairs survival in ischemia in an apoptosis-defective background

A: Western blot analysis of Beclin1, BCL-2, E1A, p53DD, and actin in *beclin1*$^{+/+}$ and *beclin1*$^{+/-}$ iBMK cell lines with and without BCL-2 expression.

B: *beclin1* haploinsufficiency impairs autophagy. *beclin1*$^{+/+}$ and *beclin1*$^{+/-}$ iBMK cells expressing BCL-2 (WB-3 and BLNB-12) were transfected with the EGFP-LC3 expression vector and at 24 hr posttransfection were subjected to 0 and 24 hr of ischemia and were monitored for membrane translocation by fluorescence microscopy. Representative fields are shown.

C: Quantitation of EGFP-LC3 translocation (% autophagy) in WB-3 and BLNB-12 in **B** following 0, 1, 2, and 3 days in ischemia.

D: *beclin1* haploinsufficiency impairs viability in ischemia only when apoptosis is inhibited. *beclin1*$^{+/+}$ and *beclin1*$^{+/-}$ iBMKs with and without BCL-2 were incubated in ischemic conditions, and viability was assessed by trypan blue staining at the indicated times.

E: Time course of morphological alterations due to *beclin1* haploinsufficiency in iBMK cells expressing BCL-2 (WB-13 and BLNB-12). *beclin1*$^{+/+}$ cells expressing BCL-2 proliferate, followed by cellular condensation, whereas *beclin1*$^{+/-}$ cells expressing BCL-2 display diminished capacity to sustain proliferation and show accelerated necrosis.

F: EM (5000×) of *beclin1*$^{+/+}$ BCL-2 (WB-13) and *beclin1*$^{+/-}$ BCL-2 (BLNB-12) following 7 days in ischemia. Note the condensed morphology of WB-13 and the vacuolated and necrotic morphology of BLNB-12.

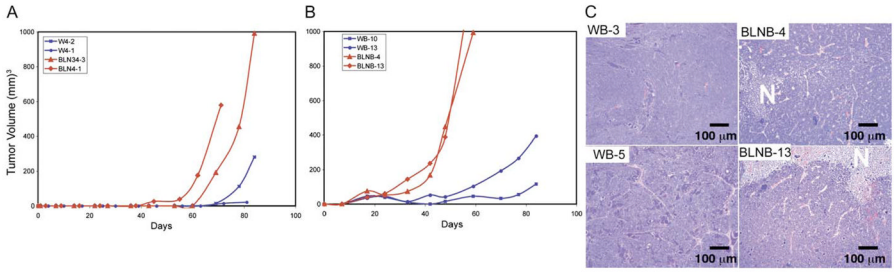

Figure 7. *beclin1* haploinsufficiency promotes epithelial tumorigenesis

A: Tumor growth kinetics of two *beclin1*$^{+/+}$ (W4-2, W4-1) and two *beclin1*$^{+/-}$ (BCLN34-3, BCLN4-1) iBMK cell lines.

B: Tumor growth kinetics of two *beclin1*$^{+/+}$, BCL-2-expressing (WB-10, WB-13) and two *beclin1*$^{+/-}$, BCL-2-expressing (BLNB-4, BCLNB-13) iBMK cell lines.

C: Histology of two *beclin1*$^{+/+}$, BCL-2 (left) and two *beclin1*$^{+/-}$, BCL-2 (right) tumors. One out of eight *beclin1*$^{+/+}$, BCL-2 tumors and six out of eight *beclin1*$^{+/-}$, BCL-2 tumors showed evidence of necrosis (N). All tumors were between 500 and 1000 mm^3 at the time of histological analysis.

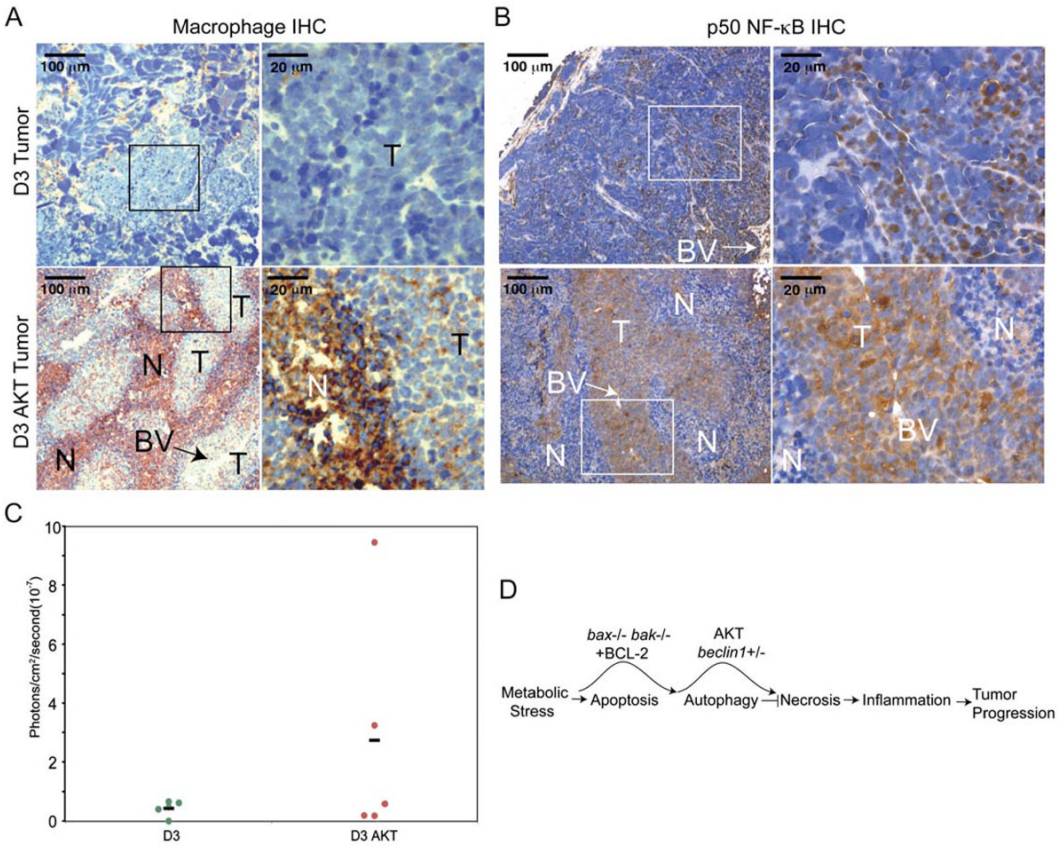

Figure 8. Tumor necrosis is associated with macrophage infiltration and cytokine and chemokine production

A: The macrophage marker Mac3 staining of D3 (B4) and D3 AKT (D5) tumors by IHC with brown staining indicating reactivity in necrotic areas (100×, insets 400×). Note the high level of reactivity in necrotic areas of D3 AKT tumors and the near absence of staining in D3 tumors.

B: IHC for p50 NF-κB as in **A** demonstrating enhanced staining in D3 AKT tumors.

C: In vivo tumor necrosis is associated with enhanced activity of the cytokine-responsive IL6 promoter. Tumors were generated subcutaneously by injecting D3 or D3AKT cells stably expressing a luciferase reporter gene under the control of three NF-κB DNA binding motifs from the IL6 promoter and monitored for in vivo promoter activation. To compare the relative luminescence signals in D3 and D3 AKT tumors, the total photon values were normalized to basal luminescence activity at day 2 postinjection and compared to that after tumor growth where tumor sizes were comparable: day 15 for D3 AKT with an average tumor volume of 88.9 mm^3, day 29 for D3 with an average tumor volume of 82.2 mm^3. The graph represents relative IL6-LUC activity from five individual tumors of each genotype with the mean indicated by the bar.

D: Model for hierarchy of death pathways and impact on tumor growth.